Scilight

Advanced Antibacterial Materials

https://www.sciltp.com/journals/aam

Article

Bacteria-Powered Photodynamic Amplification on Nano-Bio Interface for Selective Pathogen Killing and Tissue Regeneration

Jieni Fu [1,2,3], Chaofeng Wang [1], Congyang Mao [2], Hui Jiang [3], Jie Shen [4], Zhaoyang Li [3], Yanqin Liang [3], Shengli Zhu [3], Zhenduo Cui [3] and Xiangmei Liu [1,2,*]

[1] School of Health Science & Biomedical Engineering, Hebei University of Technology, Xiping Avenue 5340#, Tianjin 300401, China
[2] Biomedical Materials Engineering Research Center, Hubei Key Laboratory of Polymer Materials, Ministry-of-Education Key Laboratory for the Green Preparation and Application of Functional Materials, School of Materials Science & Engineering, State Key Laboratory of Biocatalysis and Enzyme Engineering, Hubei University, Youyi Avenue 368#, Wuhan 430062, China
[3] School of Materials Science & Engineering, the Key Laboratory of Advanced Ceramics and Machining Technology by the Ministry of Education of China, Tianjin University, Yaguan Road 135#, Tianjin 300072, China
[4] Shenzhen Key Laboratory of Spine Surgery, Department of Spine Surgery, Peking University Shenzhen Hospital, Lianhua Road 1120#, Shenzhen 518036, China
* Correspondence: liuxiangmei1978@163.com

Supplementary Materials

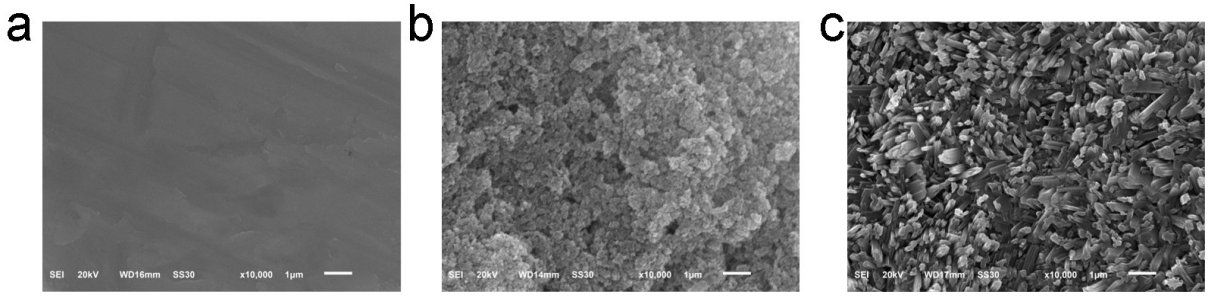

Figure S1. The SEM picture of (**a**) Ti6. (**b**) HA-Ti6. (**c**) MoS_2-Ti6.

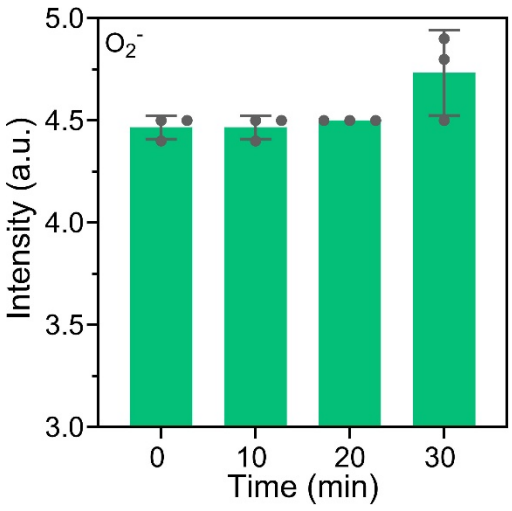

Figure S2. Absorption spectrum of TA solution.

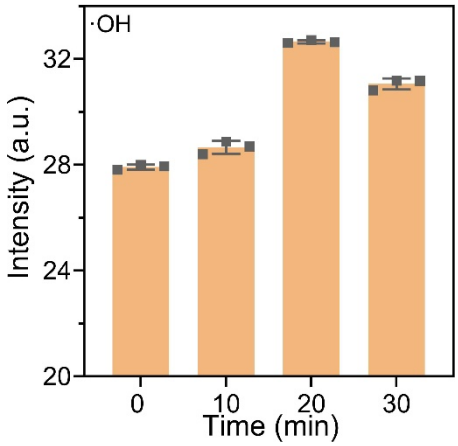

Figure S3. Absorption spectrum of NBT solution.

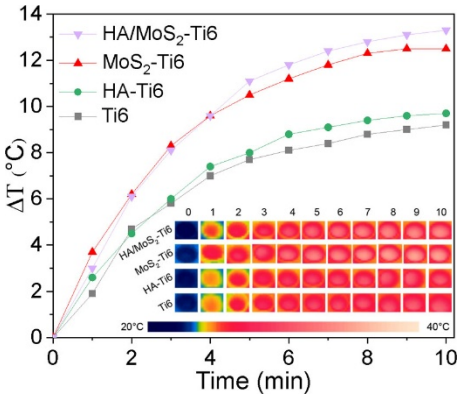

Figure S4. Photothermal heating curves of Ti6, HA-Ti6, MoS2-Ti6, and MoS2/HA-Ti6 under 660 nm irradiation for different time. The inserted pictures were infrared thermal images of the samples under 660 nm irradiation for different time.

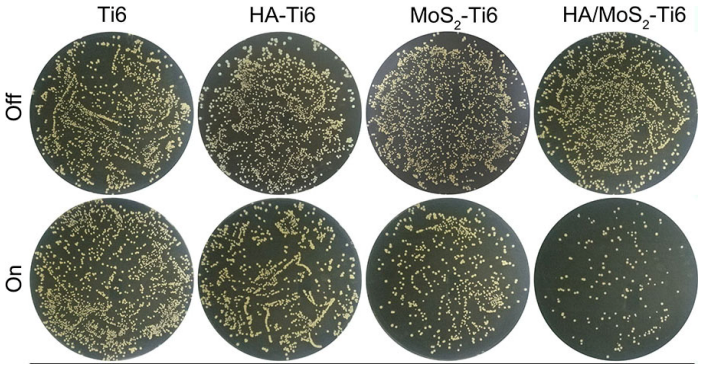

Figure S5. Spread plate results of *S. aureus*.

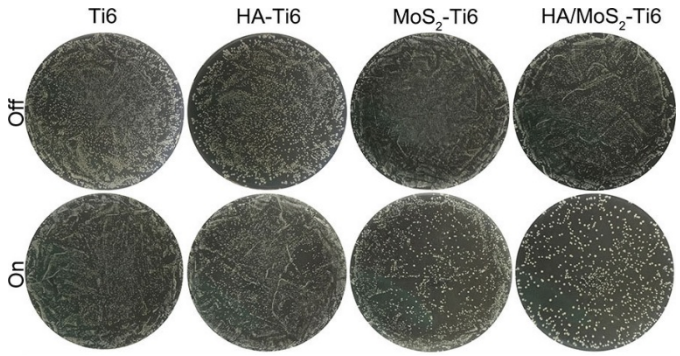

Figure S6. Spread plate results of *E. coli*.

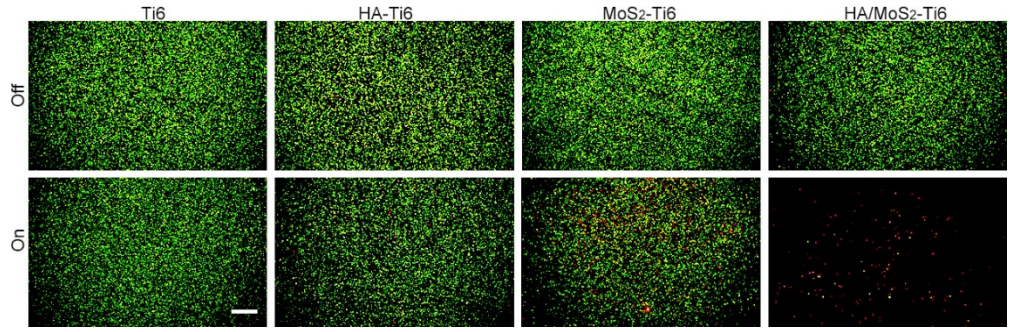

Figure S7. The fluorescent images of bacterial dead/living pictures of different samples (Ti6, HA-Ti6, MoS_2-Ti6, and HA/MoS_2-Ti6) with or without 660 nm laser irradiation.

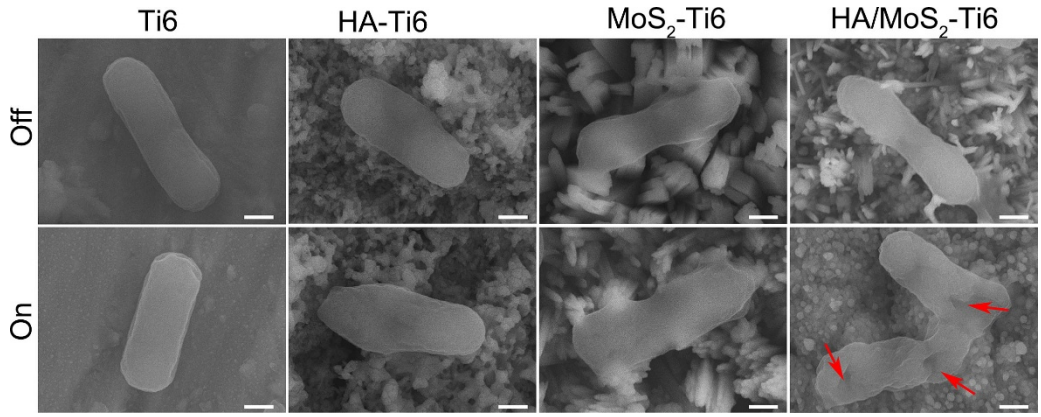

Figure S8. The bacterial SEM images of different samples (Ti6, HA-Ti6, MoS_2-Ti6, and HA/MoS_2-Ti6) with or without 660 nm laser irradiation. The scale bar is 1 μm.

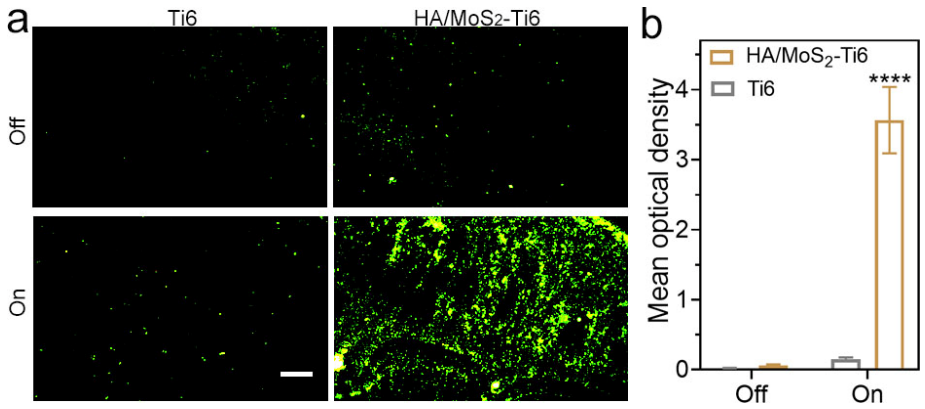

Figure S9. (**a**) The fluorescent images of *E. coli* incubated with different samples (Ti6 and HA/MoS_2-Ti6) under 660 nm laser irradiation. Intracellular ROS was stained with DCFH-DA. (**b**) The quantitative analysis of DCFH fluorescent density. n = 3 independent experiments per group, **** $p < 0.0001$. Statistical significance was calculated with one-way ANOVA with Dunnett's multiple comparisons.

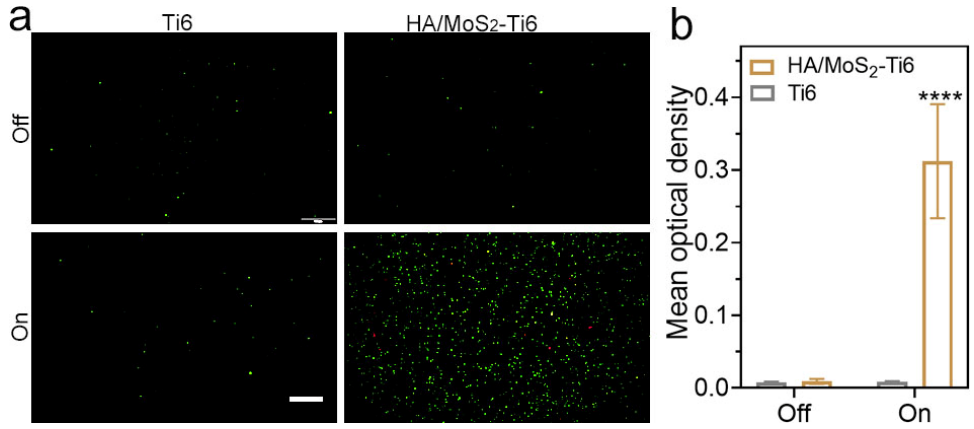

Figure S10. (**a**) The fluorescent images of *E. coli* incubated with different samples (Ti6, HA-Ti6, MoS_2-Ti6, and HA/MoS_2-Ti6) under 660 nm laser irradiation. Bacterial membrane potential was stained with DiBAC4(3). (**b**) The quantitative analysis of membrane potential fluorescent density. n = 3 independent experiments per group, **** $p < 0.0001$. Statistical significance was calculated with one-way ANOVA with Dunnett's multiple comparisons.

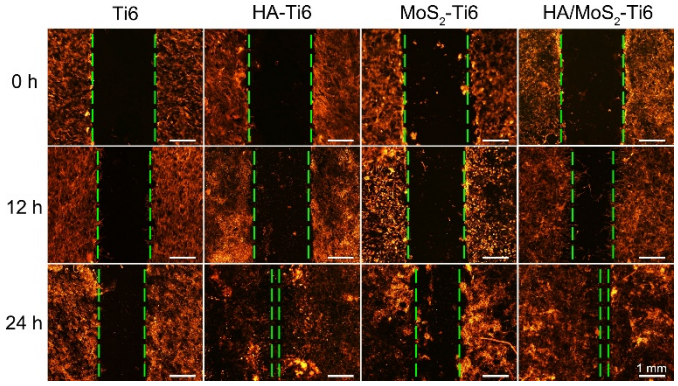

Figure S11. Fluorescence images of MC3T3-El cells at 0 h, 12 h, and 24 h after being incubated with Ti6, HA-Ti6, MoS_2-Ti6, and HA/MoS_2-Ti6. Actin was stained with red. Scale bar:100 μm.

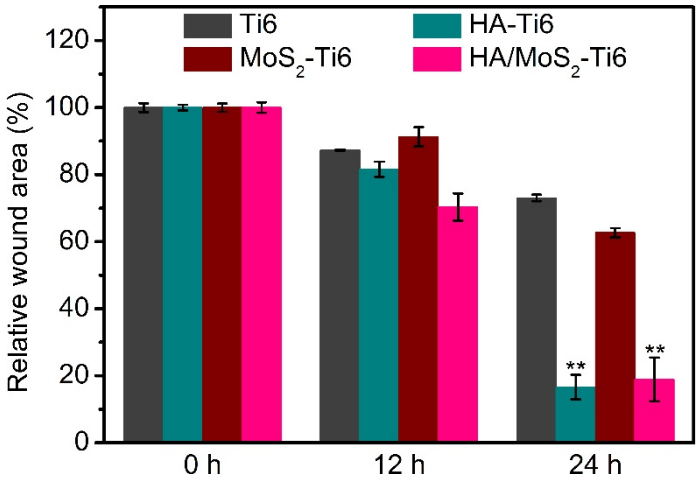

Figure S12. The quantitative analysis of MC3T3-El migration distance. ** $p < 0.01$.

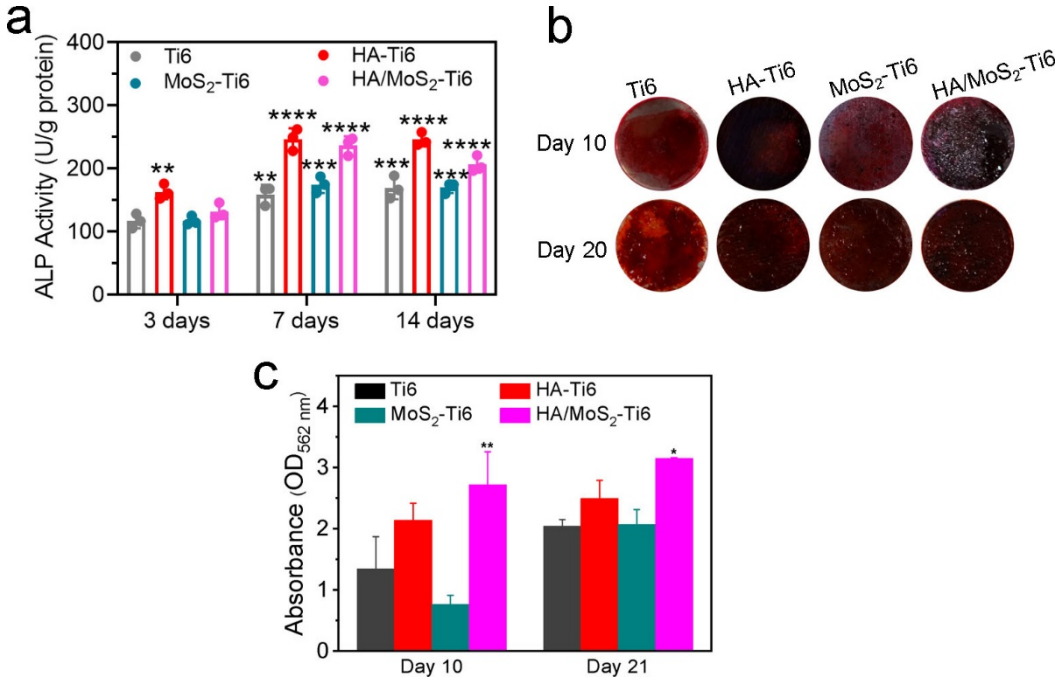

Figure S13. (**a**) ALP activity of MC3T3-E1 osteoblasts after culturing on the surface of different samples for 3 days, 7 days and 14 days. (**b**) Alizarin red staining images of different samples at 10 days and 20 days. (**c**) The quantitative analysis of ARS staining for MC3T3-El osteoblasts. Data are presented as mean ± standard deviations from a representative experiment. Error bar represents the standard deviation. n = 3 independent experiments per group, * $p < 0.05$, ** $p < 0.01$, *** $p < 0.001$, **** $p < 0.0001$. Statistical significance was calculated with one-way ANOVA with Dunnett's multiple comparisons.

It is known that HA can enhance osteoblast differentiation due to its osteoconduction [38]. The ALP activities of MC3T3-E1 osteoblasts were assessed after co-culturing with HA-Ti6, MoS_2-Ti6, and HA/MoS2-Ti6 at 3 days and 7 days and 14 days (Figure S13a). After co-culturing with different samples at different time, compared with Ti6 group, the HA-Ti6 and HA/MoS_2-Ti6 groups showed higher ALP activity. MoS_2-Ti6 group presented similar ALP activity to those of Ti6 group. ARS activity of MC3T3-E1 osteoblasts was used to demonstrate the extracellular mineralization of samples [39]. Similar results were also observed in ARS assay (Figure S13b,c). The ability of extracellular mineralization in HA/MoS_2-Ti6 and MoS_2-Ti6 groups were considerably higher than Ti6 group.